



## Seismic risk assessment of ultra-high voltage bypass switches with the multiple failure modes

J.Y Wen<sup>(1)</sup>, Q. Xie<sup>(2)</sup>

<sup>(1)</sup> Ph.D. Student, Department of Structural Engineering, Tongji University, [tjtmwjy@tongji.edu.cn](mailto:tjtmwjy@tongji.edu.cn)

<sup>(2)</sup> Prof., Department of Structural Engineering, Tongji University, [qxie@tongji.edu.cn](mailto:qxie@tongji.edu.cn)

### Abstract

Bypass switches are widely used in electrical substations to switch current to the bypass during maintenance or breakdown of the main circuit. The bypass switch has two symmetrical horizontal chambers supported by an erect post insulator, and forms a T-shaped structure. The switching devices are installed inside the chambers. In the ultra-high voltage (UHV) power transmission systems, height of the UHV bypass switch is generally more than ten meters to satisfy the requirement of the insulation clearance. However, the top-installed switching devices weigh several tons, and the post insulator is relatively slender; thus, the UHV bypass switch is quite flexible, with its fundamental frequency less than 1Hz in general. From the point of the structural engineering, the UHV bypass switch is vulnerable during earthquakes, severely threatening the security of the power system and social economy. In most current available studies on the seismic performance of the bypass switch, breakage of the post insulator was set as the only failure mode. However, there are two more potential failure modes: a) Damage of the conductors and the electrical functional failure caused by the excessive relative displacement between the bypass switch and its adjacent interconnected equipment. b) Mechanical failure, residual deformation, and electrical breakdown of the switching devices. Furthermore, structural configurations of the switching devices in the open and closed configurations are different, and both these two configurations should be taken into consideration. Therefore, in order to comprehensively investigate the seismic performance and risk assessment, an elaborate finite element model of a typical UHV bypass switch with its switching devices was built. Firstly, a nonlinear time-history analysis was carried out to obtain the seismic responses of the switch in both the open and closed configurations, and it was found that the closed configuration is more dangerous. Based on the seismic responses and the electrical requirements, all the potential failure modes were classified into two assessment levels, the structural level and the functional level. In the structural level, failure happens only when the stress and residual deformations exceeding the mechanical limits; in the functional level, failure happens once the insulation clearance was not satisfied. In the risk assessment, 100 earthquake records with different characteristics were taken as the input ground motions to excite the closed configuration, and multiple strip analysis (MSA) was adopted to estimate the fragility curves of the structural level and functional level. No matter how much is the peak ground acceleration (PGA), the failure probability of the structural level is greater than that of the functional level; that is to say, the electrical functions can be ignored in the seismic qualification of the typical UHV bypass switch. Moreover, with the PGA larger than 0.3 g, the failure probability will exceed 10 %, indicating the UHV bypass switches used in the areas with high seismic intensity are not reliable in the earthquake, and the retrofit method should be employed to increase the seismic resistance.

*Keywords: bypass switch, switching devices, failure mode, risk assessment, assessment levels*



## 1. Introduction

In recent years, high voltage electrical equipment has suffered from earthquakes, and great economic losses were caused by the power outage and recovery [1]. Bypass switches, the key components of electrical substations, are used to switch current to the bypass during maintenance or breakdown of the main circuit. A typical high voltage is shown in Fig. 1. In general, a bypass switch, with two symmetrical horizontal chambers supported by an erect post insulator, forms a T-shaped structure, and switching devices are installed inside the chambers. According to the post-earthquake investigations, breakage at the root of the slender post equipment, such as the bypass switches, disconnect switches, and circuit breakers, were frequently found [2-4]. The ultra-high voltage (UHV) system is efficient in power transmissions, and has been boosted in some countries like China. However, to satisfy the requirement of the insulation clearance, height of the UHV bypass switch is generally more than ten meters, and is made from the composite material, characterized by relatively low elastic modulus. Structurally speaking, the UHV bypass switches probably produce great stress responses and large top displacement during the earthquake; thus, studies on seismic performance of the UHV bypass are worthwhile. Moreover, seismic risk assessment would be helpful to the planning of UHV substations and power transmission system.



Fig. 1 –A typical high voltage bypass switch

Several studies targeted at the seismic responses have been carried out on typical slender post electrical equipment, such as the disconnect switch [5], transformer bushing [6], and surge arrester [7]. The base isolation has been proved to be an applicable technology to improve the seismic performance of the electrical equipment. Alessandri et al. validate the isolation efficiency of a wire rope isolation system for a 420 kV circuit breaker by both the numerical and experimental methods [8, 9]. Xie et al. studied a  $\pm 800$  kV UHV bypass switch isolated by a assembled base isolation system using the wire rope isolation and viscous dampers through the shaking table testing, and found the isolation system can reduce the stress and displacement responses by about 50% [10]. In addition to the deterministic studies, some research focused on the seismic risk of electrical equipment have been also carried out. Straub and Kiureghian developed improved seismic fragility modeling based on empirical data of the damaged electrical equipment [11]. Zareei et al. investigated the failure probabilities of a 400 kV transformer using the multi strip analysis (MSA) [12]. For the UHV bypass switch, available failure data of the past earthquakes is not enough to establish the fragility modeling; thus, numerical calculation based on elaborate model is adopted as the alternate method in this study. In most previous studies of the post electrical equipment, breakage of the post insulator was set as the only failure mode. However, according to the seismic damage investigations, there are two more potential failure modes in actual: a)



Damage of the conductors and the electrical functional failure caused by the excessive relative displacement between the bypass switch and its adjacent interconnected equipment. b) Mechanical failure, residual deformation, and electrical breakdown of the switching devices. Furthermore, structural configurations of the switching devices in the open and closed states are different, and both the two configurations should be considered in the risk assessment.

In order to comprehensively investigate the seismic performance and develop a fragility model for the risk assessment, an elaborate finite element (FE) model of a typical  $\pm 800$  kV UHV bypass switch was built. In this model, the switching devices embedded in the chambers were considered. A nonlinear TMA was carried out on the model to obtain the seismic responses of the bypass switch in both the open and closed states. Based on the seismic responses and the electrical requirements, all the potential failure modes were classified into two assessment levels, the structural level and the functional level. Afterwards, 100 earthquake records with different characteristics were taken as the input ground motions in the risk assessment, and the MSA was adopted to calculate the failure probability.

## 2. Time history analysis (THA)

### 2.1 Modeling

An elaborate FE model of a  $\pm 800$  kV UHV bypass switch (shown in Fig. 2(a)) was built in this THA, and is shown in Fig. 2(b). The bypass switch consists of a steel frame, with the height of 2.5 m, three post insulators, a joint box, two horizontal chambers, two grading capacitors, and several corona rings. Total height of the bypass switch is about 15 m. The joint box, with the metal shell, is the container of the gearing, and is much stiffer than the insulators and chambers; thus, it is regarded as a mass point in the FE model. The connection among the joint box, the post insulators, and the chambers is modeled by the fixed constraint. As for the grading capacitors and corona rings, their behaviors during the earthquake are like rigid bodies. Therefore, these two components were regarded as non-structural, and only their inertial effects were considered in the FE model. The B31 beam elements were used to model the steel frame and the post insulators; meanwhile, the chambers and the switching devices were modeled by the solid elements. Constraint relationships among the modeling components are shown in Fig. 2(c).

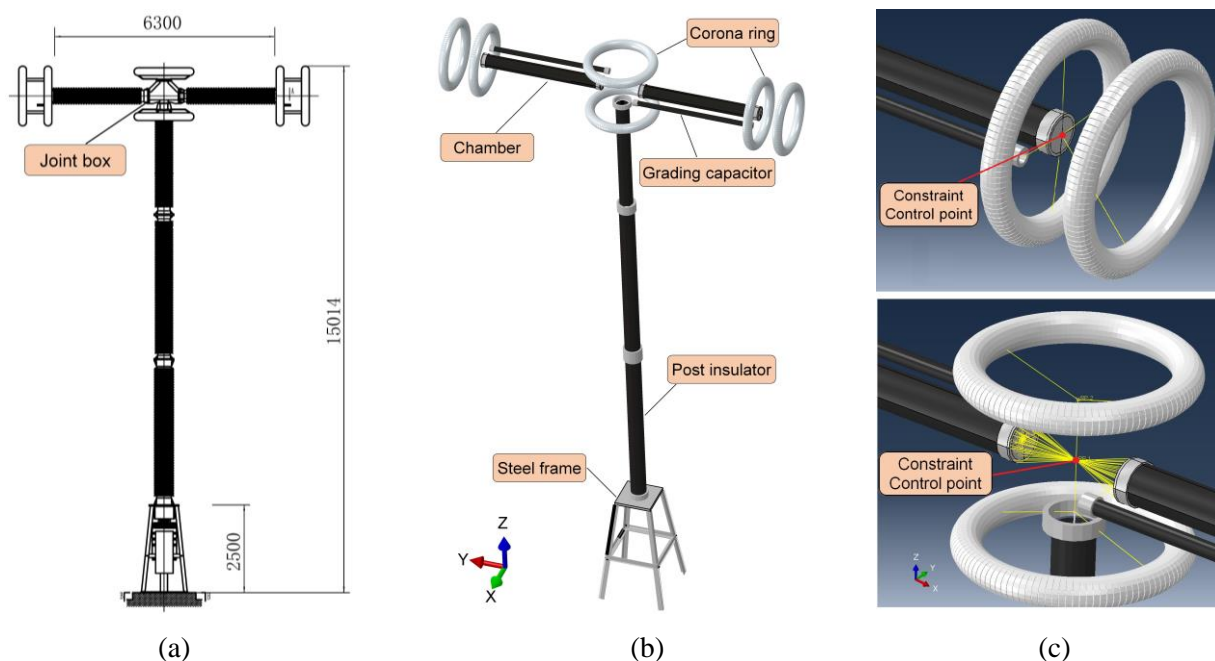


Fig. 2 –A FE model of an UHV bypass switch.



There are two main configurations of the bypass switch, i.e., the open configuration and the closed configuration, and the profiles of the left chamber with these two configurations is shown in Fig. 3. The switching devices can be divided into four parts: the fixed contact, the movable contact, the air cylinder, and the mediate contact. The support of the fixed contact and the mediate contact is fixed to the respective ends of the chamber. The movable contact is embedded in the mediate contact, and the air cylinder is jointly driven by the motion of the movable contact. The closed configuration refers to the situation when the movable contact fully stretches out to connect to the fixed contact, while the open configuration refers to that when the movable contact is detached from the fixed contact. Components of the switching devices are also shown in Fig. 3, and the dimensional parameters and material parameters were set in accordance with the design documents. To validate the FE model, eigenvalue analysis was carried out to calculate the natural frequencies of the bypass switch. Based on the actual design document, the maximum error of the first five natural frequencies of the FE model was controlled within 5 %, to ensure the effectiveness of the FE model. Discrepancy between the fundamental frequencies with the open and the closed configurations is only 0.74 %, indicating different states of the switching devices almost make no difference to the dynamic characteristics of the bypass switch. The first five modal frequencies and the vibration modes with the open configuration are listed in Table 1. The fundamental frequency is only 0.444 Hz, suggesting the bypass switch is quite flexible.

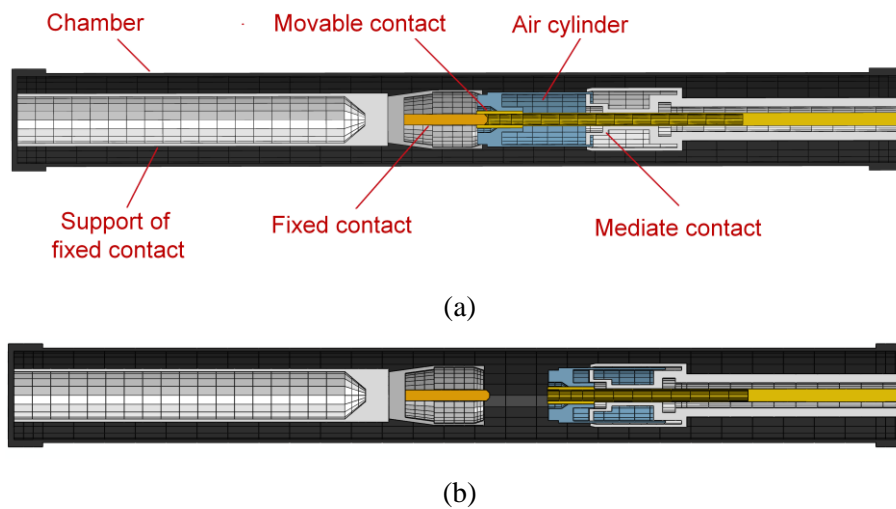


Fig. 3 –Profile of left chamber with (a) closed configuration; and (b) open configuration

Table 1 – Information of first five modes with the open configuration

Mode no.	Natural frequency (Hz)	Vibration mode
1	0.444	bend in Y direction
2	0.465	bend in X direction
3	0.938	torsion
4	1.829	bend in Y direction
5	4.497	bend in X direction



## 2.2 Input ground motion

In the THA, an artificial wave provided by the Pacific Earthquake Engineering Research Center (PEER) [13] was employed as the input ground motion in the THA. The artificial wave is the modification of the Landers earthquake record, and can envelope the required responses spectrum (RRS) in IEEE 693 standard [14] in a large frequency range. The normalized 2 % damped responses spectrum of the artificial wave and the RRS are shown in Fig.4. At the first two natural frequencies of the bypass switch (i.e., 0.444 Hz and 0.465 Hz), the artificial can well matches the RRS. As the chambers are horizontal cantilevers, the bypass switch is excited by the artificial wave in all the three directions, and the peak ground accelerations (PGA) in the X, Y, and Z direction are 0.4 g, 0.34 g, and 0.26 g, respectively.

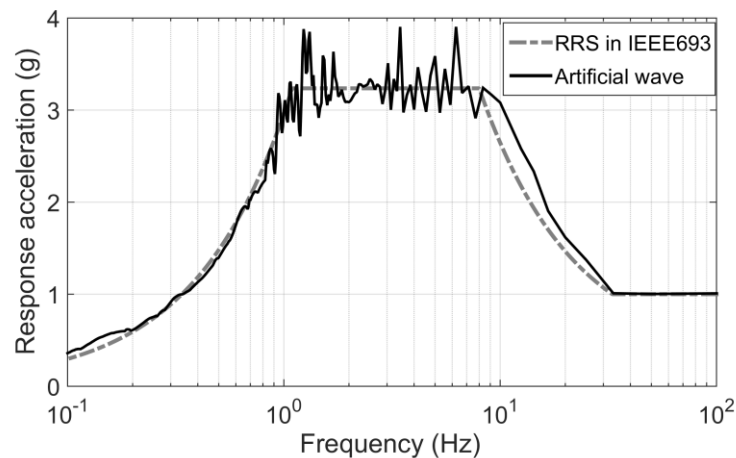


Fig. 4 –Response spectrum of input artificial wave and RRS in IEEE 693, 2% damped

## 2.3 Seismic responses

The acceleration and relative displacement responses at the top of the post insulator and the ends of the chambers are listed in Table 2. As the bypass switch is relatively flexible, amplifications of the horizontal acceleration are not obvious, while the chambers can significantly amplify the vertical acceleration. Moreover, the maximum displacement of the bypass switch, which can exceed 1000 mm, might lead to the failure of the conductor or the adjacent equipment.

Table 2 – Maximum accelerations and relative displacement at key positions

Position	Configuration	Max. acceleration (g)			Max. displacement (mm)		
		X dir.	Y dir.	Z dir.	X dir.	Y dir.	Z dir.
Top of the post insulator	open	0.53	0.38	0.26	928.0	799.9	76.8
	closed	0.54	0.40	0.26	1044.4	684.5	80.0
End of the chamber	open	0.56	0.39	0.73	956.8	818.5	322.8
	closed	0.57	0.41	0.74	1071.0	698.0	271.8

The maximum stress of the post insulators and the chambers obtained from the THA are listed in Table 3. Notably, the stress aroused by the gravity was considered in Table 3. The maximum stress of the chambers with the two configurations are similar, while stress of the post insulators with the closed configuration about



12.3 larger than that with the open configuration. At the moment when the maximum stress of the chamber occurs, the stress cloud map of the profile of the left chamber is shown in Fig. 5. In the open configuration, the maximum stress (14.92 MPa) occurs in the root of the chamber. However, in the closed configuration, the maximum stress (42.5 MPa) occurs in the rod of the movable contact, and is much greater than that of the chamber. The stress responses suggest that the stress of the post insulators should be qualified no matter what is the configuration, while stress of the switching devices should be qualified with the closed configuration.

Table 3 – Maximum stress of post insulators and chambers

Components	Open configuration	Closed configuration
Post insulator	52.97 MPa	59.46 MPa
Chamber	14.92 MPa	14.46 MPa

The ultimate stress of the composite fiberglass of the post insulators is 75 MPa, and the maximum stress of the post insulator and the chamber are about 79.3 % and 19.9 % of the ultimate stress, respectively. The rod of the movable contact is made of the copper alloy, with its yield stress of 680 MPa, and the maximum stress 42.5 MPa is only 6.3 %. That is to say, it is believed that before the breakage of the post insulator or the chambers, the switching devices behave linearly. Because the composite fiberglass is typical brittle material, seismic responses of the bypass switch will be almost linear before the structural damage, if the geometrical non-linearity. Therefore, linear calculating method can be used in the risk assessment to obtain the failure probability of the bypass switch.

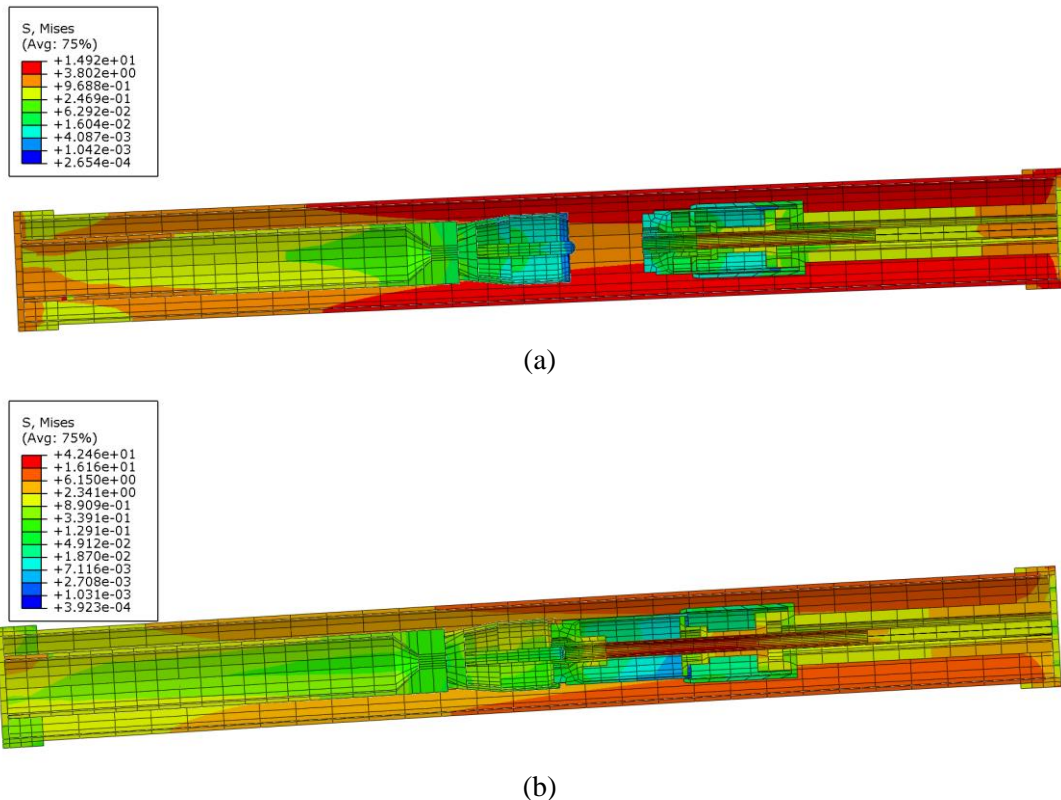


Fig. 5 – Stress cloud map, left chamber, with (a) open configuration; and (b) closed configuration



### 3. Seismic risk assessment

#### 3.1 Failure modes and assessment levels

According to the THA, stress of the post insulator and the switching devices with the closed configuration are obviously larger than those with the open configuration; thus, the closed configuration was regarded as the adverse configuration, and the risk assessment was carried out on the closed configuration. Moreover, two assessment levels were defined as follows:

a) Structural level. In this level, failure happens when the stress and residual deformations exceeding the mechanical limits. As the switching devices and the chambers are much safer than the post insulator, failure of this level actually is the damage of the post insulator, which is defined as the failure mode 1. According to the qualification guideline, if the maximum stress of the post insulator reaches 60% of the ultimate stress (i.e., the safety factor is 1.67), the failure mode 1 will happen.

b) Functional level. In this level, failure happens once the insulation clearance was not satisfied. As the insulation clearance can be classified as the inner insulation clearance (i.e., the distance between the switching devices and the interior wall of the chamber) and the outer insulation clearance (i.e., the distance between the bypass and the adjacent equipment), two failure modes are defined in the functional level. The case where the inner clearance and the outer clearance were not satisfied are defined as the failure mode 2 and mode 3, respectively. Specifically, if the relative displacement between any two components of the switching devices exceed 33 % of the original distance between them (i.e., a third of the inner insulation clearance is lost), the failure mode 2 will happen. Judgement of the failure mode 3 should take the displacement of the adjacent equipment into consideration; however, specific type of the adjacent is not determined. In the present study, a quick estimation method was adopted. The adjacent was assumed as a single degree structure with three different fundamental frequencies of 1 Hz, 2 Hz, and 3 Hz, i.e., the frequencies closed to fundamental frequencies of the general slender post electrical equipment; and the maximum displacement of the adjacent equipment under the three circumstances, denoted as  $d_{a1}$ ,  $d_{a2}$ , and  $d_{a3}$ , were calculated by the response spectrum method. The maximum displacement of the bypass switch was denoted as  $d_b$ ; thus, the relative displacement  $d_r$  is given by

$$d_r = \max\{ |d_{a1} - d_b|, |d_{a2} - d_b|, |d_{a3} - d_b| \} \quad (1)$$

When  $d_r$  exceed 33 % of the original distance between the bypass switch and the adjacent equipment, the failure mode 3 was regarded as happening.

#### 3.2 Failure probabilities

In the seismic risk assessment, 100 earthquake records provided the PEER ground motion database [15] were selected as the input ground motions of the THA, and the key maximum responses were calculated through the response spectrum method to evaluate the failure. Because the bypass switch is significantly flexible, earthquake records of the soft ground, whose shear wave velocity soil cover is less than 250 m/s. In order to obtain the fragility curve of the bypass switch, the MSA was adopted in this study. Firstly, the input ground motions were sorted into several groups according to their PGA, and the failure probabilities at different PGA levels were calculated by using the failure criteria proposed in the section 3.1. Then, based on these discrete failure probabilities, the probabilistic model of the fragility curve could be determined by the estimation methods. The failure probabilities of the bypass switch at the structural level and the functional level are listed in Table 4. It deserves mention that in the structural level, for all the input ground motions, failure of the post insulator happens prior to the failure of the chambers; while in the functional level, failure of the outer insulation clearance always happens prior to the failure of the inner insulation clearance. According to Table 4, when the PGA is less than 0.6 g, the structural failure happens before the failure of the electrical functions, with the assumptions of the failure criteria adopted in this study.



Table 4 – Failure probabilities in two different assessment levels

PGA (g)	Structural level	Functional level
0.1	0	0
0.2	0	0
0.3	0.07	0
0.4	0.33	0.12
0.5	0.47	0.26
0.6	0.73	0.41

### 3.3 Fragility curve estimation

In the section 3.2, the discrete failure probabilities in the structural and functional levels were calculated. In order to comprehensively evaluate the seismic risk in these two levels, the fragility curves were estimated through the MSA. With this method, the log-normal distribution was adopted to describe the failure probability of the bypass switch. The PGA at which the failure happens is selected as the random variable; thus, the failure probability can be expressed as

$$P(\text{Failure happens} | \text{PGA} = x) = \Phi\left(\frac{\ln x - \theta}{\beta}\right) \quad (2)$$

in which  $P(\text{Failure happens} | \text{PGA} = x)$  is the conditional probability of the occurrence of the failure, with the PGA equal to  $x$ , and  $\Phi(\cdot)$  is the standard normal cumulative distribution function,  $\theta$  and  $\beta$  are the mean value and standard deviation of  $\ln x$ . According to the discrete failure probabilities given by Table 4, the distribution parameters  $\theta$  and  $\beta$  for the structural level and functional level were estimated by the least square method, and are listed in Table 5. Based on the distribution parameters, the fragility curves of these two levels were plotted in Fig. 6. It is suggested by Fig. 6 that with the same PGA level, the failure probabilities of the structural level is always greater than that of the functional level. In other words, the structural failure happens prior to the electrical functions failure. Therefore, to estimate the seismic risk of the typical  $\pm 800$  kV UHV bypass switch, the electrical failure can be ignored. Subjected to the earthquake with the PGA less than 0.2 g, the bypass switch can be regarded as absolutely safety. However, considering the importance of the UHV power system, the PGA used for the design of the UHV electrical equipment generally is 0.3 g or 0.4 g. At the PGA level of 0.4 g, the failure the probability is closed to 40 %, indicating the bypass switch is unreliable during the earthquake. Because stress of the post insulator is the determinant of the failure, retrofit measures, such as the isolation and enlargement of the insulator section, should be applied to the conventional UHV bypass switch to reduce the stress responses.

Table 5 – Estimated values of distribution parameters

Parameters	Structural level	Functional level
$\theta$	- 0.708	0.370
$\beta$	- 0.428	0.402



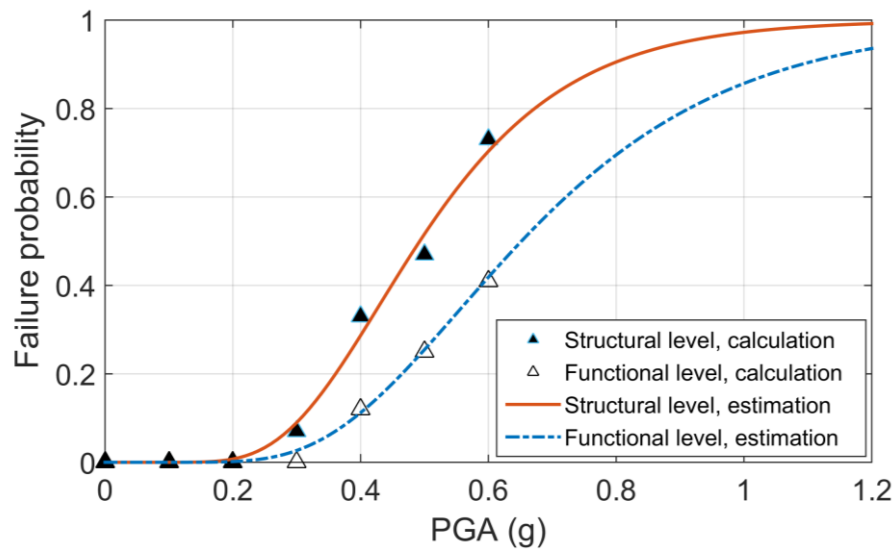


Fig. 6 – Estimated fragility curves at different levels

#### 4. Conclusion

An elaborate finite element model of a  $\pm 800$  kV UHV bypass switch with its switching devices was built, and the THA and seismic risk assessment were carried out on the model. We can draw conclusions as follows:

1. In the THA, the bypass switch with the closed and open configurations were analyzed. The bypass switch is an extreme flexible equipment, and displacement at the top can exceed 1.0 m with the 0.4 g PGA. Stress of the post insulators is predominant in both the two configurations, and the stress of the switching devices with the closed configuration is much larger than that with the open configuration. Overall speaking, the closed configuration is more dangerous during the earthquake.

2. In the seismic risk assessment, potential failure modes were classified into two assessment levels, i.e., the structural level and the functional level. Failure of the structural level is the breakage of the post insulator or the chamber; failure of the functional level is the damage of the insulation clearance. The MSA was adopted to estimate the fragility curves of these two levels. In all cases, the failure probability of the structural level is greater than that of the functional level, and the stress of the post insulator is the determinant. Therefore, in the seismic qualification of the typical UHV bypass switch, it is acceptable to not take the electrical functions into consideration. When the PGA is larger than 0.3 g, the failure probability will exceed 10 % and increase rapidly, suggesting safety of the UHV bypass switches will not be guaranteed during the severe earthquake, and the retrofit method should be employed to increase their seismic resistance.

#### 5. Acknowledgements

This study was financially supported by the National Key R&D Program, China (Grant No.2018YFC0809400) and the National Natural Science Foundation, China (Grant No. 51878508). Their support is greatly appreciated.

#### 6. References

References must be cited in the text in square brackets [1, 2], numbered according to the order in which they appear in the text, and listed at the end of the manuscript in a section called References, in the following format:

- [1] Xie Q, Zhu RY (2011): Earth, Wind, and Ice. *IEEE Power Energy Magazine*, **9** (2), 28-36.



- [2] Zhao B, Taucer F (2010): Earth, Performance of infrastructure during the May 12, 2008 Wenchuan earthquake in China. *Journal of Earthquake Engineering*, **9** (2), 28-36.
- [3] Edward CL (2013): Haiti Mw 7.0 Earthquake of January 12, 2010: Lifeline Performance. TCLEE Monograph Series, ASCE, Reston, USA.
- [4] Tang AK (2012): Tohoku Japan Earthquake and Tsunami of March 11 2011. Lifeline performance. TCLEE Monograph Series, ASCE, Reston, USA.
- [5] Moustafa MA, Mosalam (2016): Substructured dynamic testing of substation disconnect switches. *Earthquake Spectra*, **32**(1), 567-589.
- [6] He C, Xie Q, Zhou Y (2019): Substructured dynamic testing of substation disconnect switches. *Earthquake Spectra*, **35**(1), 447-469.
- [7] Li S, Tsang HH, Cheng YF, et al. (2017): Considering seismic interaction effects in designing steel supporting structure for surge arrester. *Journal of Constructional Steel*. **132**, 151-163.
- [8] Alessandri S, Giannini R, Paolacci F, et al. (2015): Seismic retrofitting of an HV circuit breaker using base isolation with wire ropes. Part 1: preliminary tests and analyses. *Engineering Structures*. **98**, 251-262.
- [9] Alessandri S, Giannini R, Paolacci F, et al. (2015): Seismic retrofitting of an HV circuit breaker using base isolation with wire ropes. Part 2: breaker using base isolation with wire ropes. Part 2: shaking-table test validation. *Engineering Structures*. **98**, 263-274
- [10] Xie Q, Yang Z, He C, et al. (2019): Seismic performance improvement of a slender composite ultra-high voltage bypass switch using assembled base isolation. *Engineering Structures*, **194**, 320-333.
- [11] Straub D, Kiureghian AD (2008): Improved seismic fragility modeling from empirical data, *Structural Safety*, **30**(4), 320-336.
- [12] Zareei SA., Hosseini M., Ghafory-Ashtiany M. (2016): Seismic failure probability of a 400 kV power transformer using analytical fragility curves, *Engineering Failure Analysis*, **70**, 273-289.
- [13] Takhirov SM, Fenves GL, Fujisaki E, et al. (2004): Input motion for earthquake simulator qualification of electrical substation equipment. *Technical Report PEER 2004/07*, Pacific Earthquake Engineering Research Center, Berkeley, USA.
- [14] Institute of Electrical and Electronics Engineers (2018): *Recommended Practice for Seismic Design of Substations*, *IEEE 693 Standard*, New York, USA.
- [15] Pacific Earthquake Engineering Research Center (2011): PEER Ground Motion Database, available at <https://ngawest2.berkeley.edu/> (last accessed 02 November 2019).